Electronic Structure of Polyvalent Metals

WALTER A. HARRISON
General Electric Research Laboratory, Schenectady, New York
(Received January 4, 1960)

A single-orthogonalized-plane-wave approximation is defined and used to construct the Fermi surfaces for face-centered-cubic and body-centered-cubic metals of valence one through four and for hexagonal-close-packed metals of valence one through three. The de Haas-van Alphen effect, cyclotron-resonance effect, and anomalous-skin effect are discussed in detail in terms of these surfaces and the deduced properties are compared with experiment where suitable experiments exist. In particular, earlier and equivalent comparisons for lead and for aluminum are reviewed, and detailed comparisons with existing experimental data on zinc and cadmium are made. It is found that the single-OPW approximation is in semiquantitative agreement with experiment in all of these cases, both as to the form of the Fermi surface and its associated effective masses. In conjunction with these studies, detailed descriptions of the apparent Fermi surfaces in zinc and cadmium are given. An extension of the method to allow experimental determination of a more precise description of the band structure is discussed, and the generalization of the method to studies of alloys is outlined.

I. INTRODUCTION

THE free-electron theory of metals has been an extremely useful theory since it was originally proposed by Drude[1] and particularly since quantum statistics were applied by Sommerfeld.[2] This theory has been extended to include a very weak lattice potential in the "nearly-free-electron" approximation[3] and profitably applied to the study of many properties of metals and alloys. More recently a "nearly-free-electron" approximation has been applied to a study of the de Haas-van Alphen effect in lead by Gold[4] and to a study of Gunnersen's[5] data on the de Haas-van Alphen effect in aluminum by the author.[6] The success of this theory has been remarkable, particularly since free-electron wave functions are certainly quite poor approximations to the true wave functions in a metal and the lattice potential is certainly not small. Within the past few years a new understanding of the reason for this success has been developing.

In a careful orthogonalized-plane-wave calculation of the band structure of aluminum, Heine[7] noted that the band energy in the first two bands is given quite closely by the free-electron value except very close to Brillouin-zone faces, suggesting that the *effective* lattice potential is weak and that in much of the zone the wave function is given fairly closely by a single orthogonalized plane wave. It has been known for some time that the effect of orthogonalizing conduction-band states to the core might be represented by a repulsive contribution to a pseudopotential,[8] but only recently has it been pointed out, by Phillips and Kleinman,[9] that this repulsive contribution may, to a large extent, cancel the core potential itself, making the effective net potential considerably weaker than might at first be expected. Cohen[10] has pointed out that this cancellation is not fortuitous and that it may be expected in metals under fairly general circumstances.

The possibility that the effective lattice potential entering the OPW approximation is weak suggests a succession of approximations which might be applied to the metal. One would first construct plane waves, suitably orthogonalized to the core states. In this representation one could then calculate the matrix elements of the Hamiltonian; the off-diagonal elements arise only from the effective potential and are expected to be small. They will in some cases, however, connect degenerate states, so that if we wish to *treat* these elements as small we must first transform to a new representation in which the off-diagonal elements connecting nearly degenerate states vanish. It will be seen in Sec. II that this transformation changes the connectivity of the bands but does essentially nothing else. The single orthogonalized plane waves in the new representation form the zeroth order of approximation, and the lattice potential does not enter it explicitly, except possibly by introducing deviations of the diagonal elements from free-electron values; we call this the single-OPW approximation. In successive steps in the approximation we would introduce the off-diagonal elements which enter most strongly, thus mixing successively more plane waves to form the approximate eigenstates. Our hope is, of course, that the initial step, the single-OPW approximation, will give a good description of the band structure.

This is apparently not the case in some of the monovalent metals, notably lithium and copper. In both of these cases the energy gaps at zone faces appear

[1] P. Drude, Ann. Physik **1**, 566 (1900).
[2] A. Sommerfeld, Z. Physik **47**, 1 (1928).
[3] See, for example, N. F. Mott and H. Jones, *The Theory of the Properties of Metals and Alloys* (Dover Publications, New York, 1958), p. 59.
[4] A. V. Gold, Phil. Trans. Roy. Soc. (London) **A251**, 85 (1958).
[5] E. M. Gunnersen, Phil. Trans. Roy. Soc. (London) **A249**, 299 (1957).
[6] W. A. Harrison, Phys. Rev. **116**, 555 (1959).
[7] V. Heine, Proc. Roy. Soc. (London) **A240**, 340 (1957).
[8] A review of the many contributions to this point of view is given by J. C. Phillips, Phys. Rev. **112**, 685 (1958).
[9] J. C. Phillips and L. Kleinman, Phys. Rev. **116**, 287 (1959).
[10] M. H. Cohen (private communication).

to be large, and the Fermi surfaces may be badly distorted. Cohen and Heine[11] have noted that though a single OPW may be satisfactory in some of the band, two are needed in important regions near zone faces. Using essentially a two-OPW approximation, they have developed a theory of the monovalent metals and their alpha-phase alloys. In spite of this complication in the monovalent metals, the success of the nearly-free-electron approximation in lead and aluminum leads us to retain the hope that the *single*-OPW approximation will give a good description of main features of the band structure in the polyvalent metals.

The author undertook a detailed analysis of aluminum, which appears in the preceding paper, in order to determine the sense in which the single-OPW approximation may be a good representation of a particular metallic band structure. As a first step, a crude band calculation was made by interpolating the self-consistent calculations of Heine.[12] Constant energy surfaces were obtained and compared with the available experimental knowledge of these surfaces. The calculated surfaces appeared to be quantitatively consistent with the experimental results, except with respect to cyclotron and specific-heat masses which were in error by a factor of two. The surfaces calculated, then, were regarded as a reasonable approximation to the "true band structure," though only semiquantitative with respect to masses, and were compared with the single-OPW approximation. The several sheets of Fermi surface which were obtained with the single-OPW approximation strongly resembled the corresponding sheets from the band calculation. Ridges which were sharp in the single-OPW surfaces became rounded in the more complete calculation, and there was some distortion in the regions of these ridges. In spite of such distortions, the single-OPW approximation was in semiquantitative agreement with the band calculation, and therefore with experiment, in its values for the various parameters which determine the electronic properties.

Thus we find that the single-OPW approximation provides a very simple semiquantitative theory of the band structure of aluminum. It is not clear, of course, that this approach will be so successful if applied to other metals, but the simplicity of the scheme and the general success that has been met by the "nearly-free-electron" approximation, as well as the plausibility of a weak pseudopotential, suggest that a generalization to other polyvalent metals may be justified.

The primary purpose of this paper is to apply this method to a series of metals, to deduce electronic properties in terms of the method, and to compare the results with experiment wherever possible in order to determine experimentally the range of validity of the method. The application to zinc and cadmium will be of considerable interest in itself by clarifying the band structure of these metals.

[11] M. H. Cohen and V. Heine, Suppl. Phil. Mag. **7**, 395 (1958).
[12] V. Heine, Proc. Roy. Soc. (London) **A240**, 361 (1957).

II. THE SINGLE-OPW APPROXIMATION

In the preceding paper we defined the single-OPW approximation in terms of the pseudopotential approximation of Phillips,[8] but we may clarify its significance by defining it here in slightly more general terms. We assume the existence of a one-electron Hamiltonian for the crystal:

$$H=\mathbf{p}^2/2m+V(\mathbf{r}), \tag{1}$$

where V is the self-consistent potential, not to be confused with the pseudopotential of Phillips. We construct the core states as before and define approximate conduction-band states $\psi_\mathbf{k}$ to be plane-waves orthogonalized to the core states and to each other. We may define the Hamiltonian matrix in the representation of these wave functions and, as before, there are no off-diagonal elements connecting core states and conduction-band states, so we consider only the conduction-band matrix. The diagonal elements $T_\mathbf{k}$ will be independent of the direction of $\mathbf{k}$ if the core potentials are spherically symmetric, if the core states do not overlap, and if the orthogonalization of plane-wave states differing by a reciprocal-lattice vector has not introduced appreciable anisotropy; we make these assumptions. The off-diagonal elements, $(\psi_{\mathbf{k}'},V(\mathbf{r})\psi_\mathbf{k})$, will connect only states differing in wave number by a reciprocal lattice vector, since $V(\mathbf{r})$ has the translational periodicity of the lattice. These off-diagonal elements must be equal to the corresponding elements of Phillips' pseudopotential since they are to give rise to the same gaps in the energy bands; the scheme becomes equivalent to that of Phillips if we replace $T_\mathbf{k}$ by the free-electron kinetic energy and use the off-diagonal elements as adjustable parameters. We will not make such an approximation at this point, but simply note that we expect these elements to be small.

The energy of a particular state will be given by $T_\mathbf{k}$ with corrections arising from the off-diagonal elements. By standard perturbation theory we can see that these corrections will be second order in the off-diagonal elements and small, except where two nearly-degenerate states are connected by an off-diagonal element. For a lattice with a single atom per unit cell this will occur for any set of nearly-degenerate states which differ in wave number by a reciprocal lattice vector; in a lattice with more than a single atom per unit cell, such as the hexagonal-close-packed lattice, some of these off-diagonal elements may be required to vanish by symmetry.

The condition for the off-diagonal elements to become important is the existence of two states $\psi_\mathbf{k}$ and $\psi_{\mathbf{k}-\mathbf{K}}$ such that $T_\mathbf{k}=T_{\mathbf{k}-\mathbf{K}}$, or $\mathbf{k}^2=(\mathbf{k}-\mathbf{K})^2$ since $T_\mathbf{k}$ is isotropic. Here $\mathbf{K}$ is a reciprocal lattice vector corresponding to nonvanishing matrix elements. This is just the condition determining a Brillouin-zone face in

band-structure language or determining a Bragg-reflection plane in free-electron language. In the region of such a plane we must treat the interaction between the states exactly. Let V_K be the appropriate off-diagonal matrix element; the eigenstates have the form $A_k\psi_k+A_{k-K}\psi_{k-K}$, where the A_k satisfy the condition,

$$\{\tfrac{1}{2}(T_{k-K}-T_k)\pm[\tfrac{1}{4}(T_{k-K}-T_k)^2+V_K^*V_K]^{\frac{1}{2}}\}A_k = V_KA_{k-K}$$

obtained by diagonalizing the two-by-two matrix. This corresponds to the transformation indicated in the introduction. Choosing a particular sign of the $\pm$, we see that as $\mathbf{k}$ moves through the region where T_k and T_{k-K} cross, A_k rapidly drops from one to zero (if the wave function is normalized suitably) while A_{k-K} rises from zero to one. This means that if we follow a state continuously as we move across one of the Bragg-reflection planes, the state changes from one of the type ψ_k to one of the type ψ_{k-K}, the distance over which this transition occurs depending upon the magnitude of V_K. As we make the V_K become small, the region of transition shrinks, and the only important effect of the potential is the alteration of the connectivity of the energy surfaces at Bragg-reflection planes. All other effects of the V_K become small as V_K becomes small and are neglected.

This, then, defines the single-OPW approximation. The constant-energy surfaces are spheres with connectivity modifications at the Bragg-reflection planes. The determination of these surfaces is quite straightforward. In particular, since we can calculate the radius of the sphere which will contain a given volume of wave-number space, and therefore a particular number of electronic states, the determination of the *Fermi* surface is a strictly geometrical problem; the only information which we require is the crystal structure and the valence of the metal. In developing this picture we have assumed that there exists a self-consistent one-electron Hamiltonian of the form of Eq. (1), that the potential $V(\mathbf{r})$ is made up of spherically-symmetric potentials around the atoms, that the core states do not overlap, and that the matrix elements between single OPW's are small. If we wish to evaluate effective masses, we must know how the energy varies from surface to surface; that is, we must know how T_k varies at the Fermi surface. In the treatment that follows we will assume the free-electron variation $dT_k/d\mathbf{k}=\hbar^2\mathbf{k}/m$.

It is of interest to examine the behavior of electrons from this point of view. The states of an electron of a particular energy, E, lie on a sphere in wave-number space of radius $k=(2mE/\hbar^2)^{\frac{1}{2}}$. As an electron moves on this energy surface (as it will under the influence of a magnetic field), it moves continuously except where the surface intersects Bragg-reflection planes and at these points it jumps to a point on the surface which lies a reciprocal-lattice vector away. We would say that in this representation, the electron trajectories in wave-number space are discontinuous.

It will turn out that this is the representation of the electronic states which is most convenient when the details of the cyclotron-resonance behavior or of the anomalous skin effect are considered. For most applications, however, another representation, the reduced-zone scheme, is preferable. It is known[13] that all of wave-number space may be mapped into the first Brillouin zone by translations by reciprocal-lattice vectors. Thus the constant-energy sphere described above is translated by segments into the central zone. Since all points differing by a reciprocal lattice vector are translated into the same point, a Bragg reflection is represented by a cusp in the wave-number trajectory, but no discontinuity. It should be noted that the same reduction can be made to a reduced zone which is not centered on a reciprocal-lattice point. If it is centered on some point other than a reciprocal-lattice point, however, the bands within the zone will have a symmetry appropriate to its central point rather than to the lattice as a whole. The center of the constant-energy sphere is required to lie on a reciprocal-lattice point by the definition of the reciprocal lattice.

The construction of constant-energy surfaces in the reduced-zone scheme may be greatly simplified by noting that when a segment of a sphere centered on a reciprocal-lattice point is translated by a reciprocal-lattice vector, it becomes the segment of a sphere centered on another reciprocal-lattice point.[14] Thus all of the segments of the constant-energy surface in the reduced zone may be obtained simply by constructing spheres around every point of the reciprocal lattice.

In going from the extended-zone scheme, in which the energy is a single-valued function of wave number, to the reduced-zone scheme, in which the energy is many-valued, we must sort out these various segments and assign them to their appropriate bands. In lattices with a center of symmetry the intersection of any two spheres (of the same energy) corresponds to the satisfaction of a Bragg condition so the constant-energy surface corresponding to a particular band changes spheres at the intersection, and surfaces from different bands cannot cross. Under these circumstances, it can be seen that if we construct spheres corresponding to a particular energy, the surface corresponding to the first band will be the surface surrounding the volume which lies within one or more spheres; the second-band surface surrounds the volume which lies within two or more spheres, etc. The bands defined in this manner will never cross, and electron states will vary continuously within each band. A state which lies on one face of the reduced zone will be equivalent to one which lies on the opposite face and corresponds to the same band. Thus if we move from state to state analytically,

[13] See, for example, F. Seitz, *Modern Theory of Solids* (McGraw-Hill Book Company, Inc., New York, 1940), Chap. 8.

[14] This scheme was used by the author in reference 6 where a two-dimensional example is described in detail.

i.e., as we follow an electron trajectory, we will never leave the band in which we start.[15]

In lattices such as hcp, which have more than one atom per unit cell, the situation is not so simple. Then the matrix elements corresponding to certain Bragg-reflection planes vanish; notably those which bound the central Brillouin zone in the direction parallel to the c axis. Any electron following a trajectory which crosses such a plane takes an electron from one band to another. It is possible to consider a larger "reduced zone" (in the case of hcp, one of twice the volume of that of the hexagonal lattice) such that a trajectory never leaves the combined band in which it starts,[15] and such that a trajectory which crosses a face of the combined zone reappears on the opposite face in the same band. In order to construct the constant-energy surfaces in such a case, one again constructs spheres around each reciprocal-lattice point, but notes that the constant-energy surfaces do not change spheres at an intersection when the centers of the two spheres differ by a reciprocal-lattice vector for which the matrix element vanishes. Each section of the single-OPW sphere appears twice in the combined zone but is drawn as a constant-energy surface only once. This requires some care in the construction, but by following appropriate trajectories along the constant-energy surfaces, it is possible to sort out the surfaces. In the hcp lattice, the only reciprocal lattice vector of interest for valences through four, which has a vanishing matrix element, is the shortest one parallel to the c axis.

The constant-energy surface which is of most interest in a metal is, of course, the Fermi surface. Thus we select a single-OPW sphere which has a volume large enough to contain the valence electrons (one-half the volume of the reduced zone times the valence times the number of atoms per cell) and construct constant-energy surfaces. It is convenient as a first step to select a plane in the Brillouin zone and draw in the intersections of the spheres centered at various reciprocal-lattice points with this plane (these are simply circles). With the aid of such figures, it is possible to draw up the surfaces in three dimensions.

The Fermi surfaces for face-centered-cubic and body-centered-cubic metals of valence one through four have been drawn up by Warner[16] at our laboratory, and are shown in Figs. 1 and 2. In addition, he drew the surfaces for a hexagonal-close-packed lattice of ideal c/a ratio for valence one through three, shown in Fig. 3. Such figures are of considerable value in isolating the features which may be important in a particular phenomenon. Detailed dimensions for these and for related structures are best found by reconstructing the intersections of these surfaces with various planes in the zone.

Armed with this concrete, though approximate, picture of the Fermi surfaces, we may proceed to consider the expected electronic properties of these metals.

III. ELECTRONIC PROPERTIES

Before considering various electronic properties in detail, it is desirable to summarize the aspects of the electronic structure each emphasizes. We look first at the de Haas-van Alphen effect, the Azbel'-Kaner effect, and the magnetoacoustic absorption, all of which depend upon the application of a dc magnetic field.

The motion of an electron in wave-number space under the influence of a magnetic field is given by[17]

$$\hbar\partial\mathbf{k}/\partial t=-(e/c)\mathbf{v}\times\mathbf{H}, \tag{3}$$

where $\mathbf{v}$ is the velocity of a wave packet in real space and is given by $(1/\hbar)\partial E/\partial\mathbf{k}$. It is seen that the component of $\mathbf{k}$ parallel to the field is independent of time and that energy is conserved. Therefore, the trajectory in wave-number space is given by the intersection of a constant-energy surface and a plane perpendicular to the magnetic field, there being a distinct orbit for each such intersection. In the three oscillatory phenomena under consideration, each orbit will contribute an oscillatory term to the effect. The observed oscillations, then, have periods corresponding to regions of the Fermi surface which give extremal periods since they are heavily weighted. There may be a further condition relevant to the Azbel'-Kaner effect, which will be discussed later.

The period of a de Haas-van Alphen oscillation is determined by the area of the electron orbits in wave-number space in the region of the Fermi surface giving rise to the oscillation. The period is related to that area by

$$\Delta(1/H)=2\pi e/c\hbar A, \tag{4}$$

in Gaussian units, as can readily be obtained by applying the Bohr-Sommerfeld quantization rule to the orbits in the field[18] as determined from (3). Thus, measurements of the periods of the de Haas-van Alphen oscillations give measurements of various cross-sectional areas of the Fermi surface.

The Azbel'-Kaner effect (cyclotron resonance in metals), on the other hand, measures the frequency of electron orbits in the field.[19] By performing a time

[15] This is not strictly true. There exist lines of contact between adjacent bands across which the wave functions change continuously from one band to another. In the single-OPW approximation these will lie on zone edges (as may be seen for face-centered-cubic lattices in the preceding paper by letting the potential go to zero). Such lines are not important physically since for any fixed set of applied forces the total volume of wave-number space comprised by trajectories which cross these lines is zero.

[16] Now at the Department of Mathematics, Massachusetts Institute of Technology, Cambridge, Massachusetts.

[17] See, for example, W. Shockley, *Electrons and Holes in Semiconductors* (D. Van Nostrand Company, Inc., New York, 1950).

[18] For a discussion of this simple approach, see R. G. Chambers, Can. J. Phys. **34**, 1395 (1956).

[19] M. Ia. Azbel' and E. A. Kaner, J. Exptl. Theoret. Phys. (U.S.S.R.) **30**, 811 (1956) [translation: Soviet Phys.—JETP **3**, 772 (1956)] and J. Exptl. Theoret. Phys. (U.S.S.R.) **32**, 896 (1957) [translation: Soviet Phys.—JETP **5**, 730 (1957)].

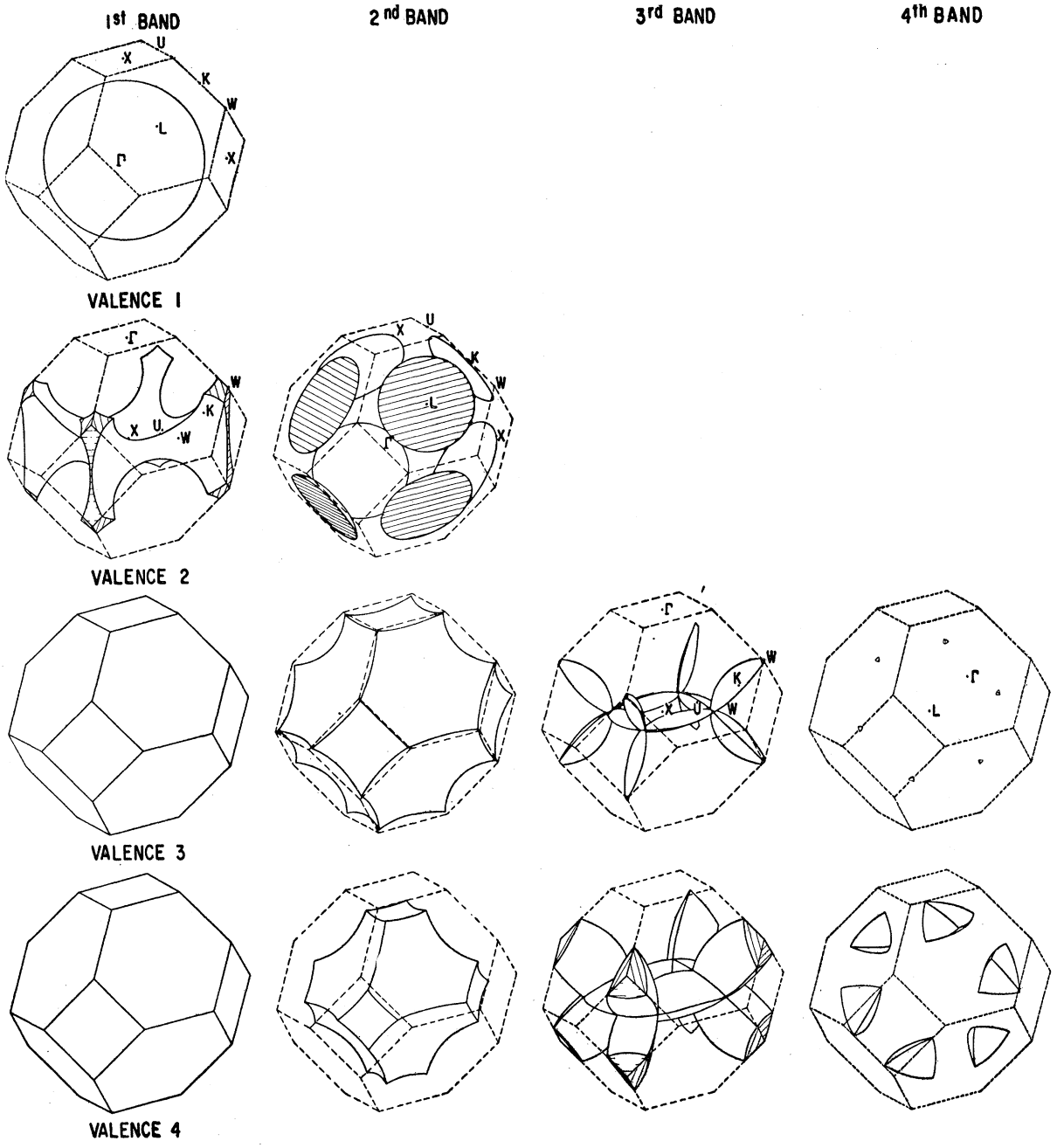

FIG. 1. Fermi surfaces of face-centered-cubic metals according to the single-OPW approximation. Note that several reduced zones are centered on positions other than Γ. Regions with convex surfaces are occupied; those with concave surfaces, unoccupied. Valance 3 and 4 correspond to aluminum and lead, respectively. Construction by F. W. Warner, III.

integral around the orbit and applying (3), we see that the orbit frequency is related to the band structure by

$$\omega_c = (2\pi eH/\hbar^2 c)/(\partial A/\partial E)_{k_H},$$

where $(\partial A/\partial E)_{k_H}$ is the rate of change of the orbit area in wave-number space in a plane perpendicular to **H** as the energy is changed. It is customary to define a cyclotron mass in terms of this frequency by $\omega_c = eH/m^*c$; then the period of the oscillation is

$$\Delta(1/H) = e/c\omega_c m^*, \tag{5}$$

with $m^* = \hbar^2(\partial A/\partial E)_{k_H}/2\pi$, in Gaussian units. Thus cyclotron resonance gives information with respect to $dE/d\mathbf{k}$ mixed with information about the geometry of the surface. An equivalent determination of the cyclotron mass may be made in terms of the temperature

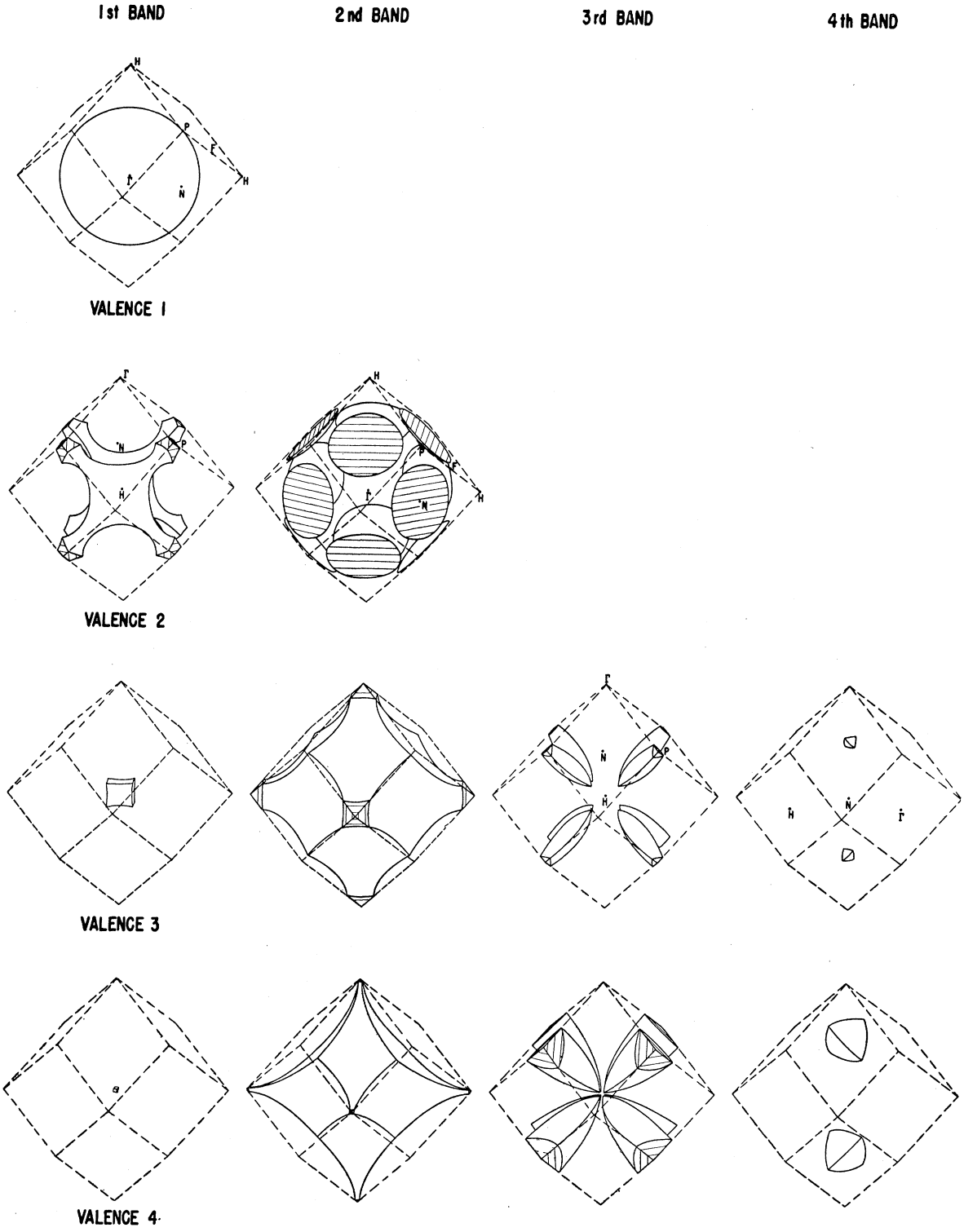

FIG. 2. Fermi surfaces of body-centered-cubic metals according to the single-OPW approximation. Note that several reduced zones are centered on positions other than Γ. Regions with convex surfaces are occupied; those with concave surfaces, unoccupied. Valance 2 corresponds to barium. Construction by F. W. Warner, III.

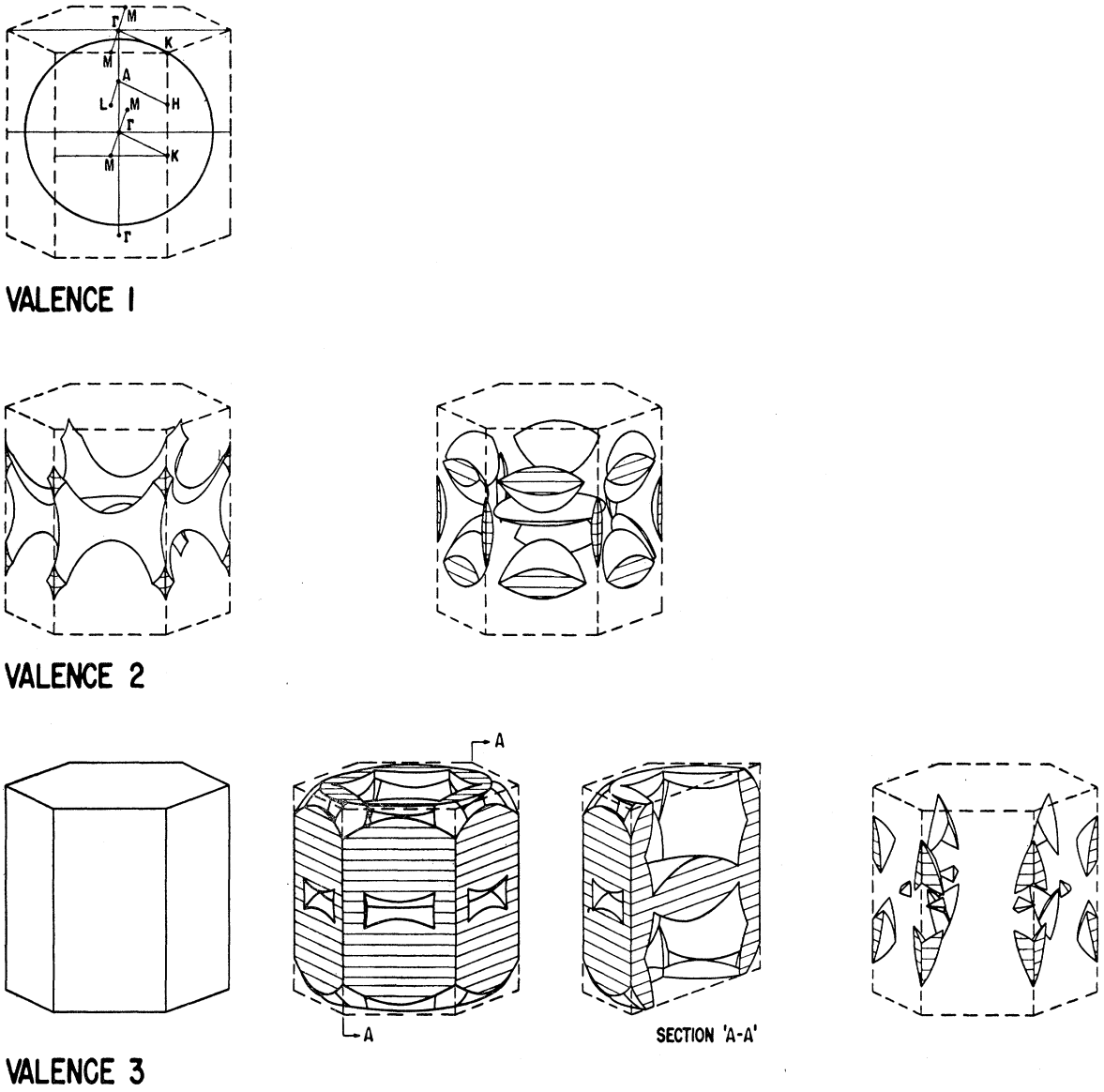

FIG. 3. Fermi surface of hexagonal-close-packed metals of ideal c/a ratio according to the single-OPW approximation. Note that the reduced zone for valence 2 is centered at the point which lies at the center of a hexagonal face of the zone as drawn for valences 1 and 3. Zinc and cadmium are represented by valence 2; thallium by valence 3. Construction by F. W. Warner, III.

dependence of the amplitudes of the de Haas-van Alphen oscillations.

Oscillations in the ultrasonic attenuation as a function of magnetic field may correspond to coincidences in the orbit dimensions [in real space, or by use of (3) indirectly in wave-number space] with the sound wavelength.[20] This effect should, in principle, give the most direct information about the shape of Fermi surfaces, but well-defined oscillations have been reported only in copper,[21] bismuth,[22] tin,[23] and in aluminum.[24]

[20] This effect, originally proposed by A. B. Pippard [Phil. Mag. 2, 1147 (1957)] has been confirmed by extensive theoretical treatments by T. Kjeldaas and T. Holstein, Phys. Rev. Letters 2, 340 (1959) and by M. H. Cohen, M. Harrison, and W. A. Harrison [Phys. Rev. **117**, 937 (1960)].

[21] R. W. Morse and J. D. Gavenda, Phys. Rev. Letters 2, 250 (1959). The period of these oscillations has been confirmed by B. W. Roberts (private communication).

[22] D. H. Reneker, Phys. Rev. **115**, 303 (1959).

[23] T. Olsen and R. W. Morse, Bull. Am. Phys. Soc. 4, 167 (1959).

[24] B. W. Roberts, Bull. Am. Phys. Soc. 4, 423 (1959).

For the orientations used in the copper experiment, the periods should correspond to a measurement of the radius of the Fermi surface along a (100) direction. These measurements correspond to a radius of 0.63, in units in which the distance from the center of the zone to the center of the square face is one. This is smaller by 20% than the value given by Pippard[25] and the value obtained with a single-OPW sphere (the two being comparable). If we assert that the Fermi surface cannot extend beyond this measured radius, we conclude that the Fermi surface must lie within a cube, the edge of which is 1.27 in our units. Such a cube has a volume about equal to that required by one electron per atom and the volume available to the electrons is even further reduced by truncating the cube to fit it in the zone. We conclude that there is some difficulty in interpreting the results, and there is uncertainty in the use of the method as long as this discrepancy remains uninterpreted. Because of this, because the data on polyvalent metals are limited, and because the significance of pictures such as Figs. 1, 2, and 3 in any attempted interpretation of data is quite clear, we will not discuss the effect any further.

In addition to these three phenomena, which depend upon the application of a magnetic field, the anomalous skin effect and the electronic specific heat give information about the electronic structure, but in a somewhat less direct form than the phenomena discussed above.

The measurement of surface impedance in the anomalous limit gives information about the curvature of the Fermi surface perpendicular to a line which runs around the Fermi surface and is the locus of points corresponding to vanishing velocity perpendicular to the specimen surface.[26] In particular, let the specimen surface lie in an x-y plane with x and y chosen along principal axes of the surface-resistance tensor. We define r_y to be the radius of curvature of an intersection of the Fermi surface with the plane k_y=constant at the points where the intersection is parallel to the z direction. Then the surface resistance in the x direction is given by[25]

$$R_x=\frac{\sqrt{3}}{2}\left(\frac{\pi\omega^2\hbar^3}{e^2\int|r_y|\,dk_y}\right)^{\frac{1}{3}}, \tag{6}$$

the integration being taken over all such points on the Fermi surface. Thus the result is not complicated by a dependence on the gradients of E with respect to $\mathbf{k}$ nor by effects of scattering. However, the rather complicated dependence upon the shape of the surface makes the data difficult to interpret and the necessity of preparing a new specimen for each point makes the data difficult to obtain.

[25] A. B. Pippard, Phil. Trans. Roy. Soc. (London) **A250**, 325 (1957).

[26] A. B. Pippard, Proc. Roy. Soc. (London) **A224**, 273 (1954) and E. H. Sondheimer, Proc. Roy. Soc. (London) **A224**, 260 (1954).

Finally, the electronic specific heat at low temperatures, γT, gives a measure of the total density of states at the Fermi surface. γ is related to the band structure by

$$\gamma=\frac{k^2}{12\pi}\frac{dV}{dE}, \tag{7}$$

where k is the Boltzmann constant, and dV/dE is the change in volume in wave-number space of the Fermi surface with change in energy. This involves a summation of contributions over the entire Fermi surface and gives the least-detailed information of the phenomena considered. It is clear that the change in connectivity of the single-OPW sphere brought about by the lattice potential does not affect the electronic specific heat, so in this approximation only the form of the single-OPW kinetic energy, $T_{\mathbf{k}}$, enters; i.e., the value of $dT_{\mathbf{k}}/d\mathbf{k}$. Since this quantity also enters the cyclotron mass through $(\partial A/\partial E)_{k_H}$, the measured electronic specific heat is of interest in connection with the analysis of the cyclotron masses, and we will discuss it only in that connection in what follows. The introduction of a finite lattice potential may modify the electronic specific heat appreciably in some cases, but as was pointed out in the preceding paper, this effect may be much smaller than at first expected.

We may now proceed to consider these phenomena in the light of what we expect from the single-OPW approximation and what is found experimentally.

1. de Haas-van Alphen Effect

It has been demonstrated[6] that de Haas-van Alphen data generally are not sufficiently complete to allow one to deduce the Fermi surface; it has been shown, in particular, that quite a wide variety of surfaces are consistent with data which would appear to be reasonably complete. On the other hand, they have proven to be the best source of information for filling in the details of the surface once its general shape has been postulated. This is just the situation which calls for an approximate band theory such as the single-OPW approximation.

The best representation of the band structure for this purpose is that in which the electron trajectories are continuous; that is, the representation illustrated in Figs. 1 through 3. As we have indicated, the appropriate analysis of data in lead and aluminum has been made, and we will summarize the findings with only minor modifications. We will then proceed to cadmium and zinc for which sufficient data exist to enable the analysis, but for which this analysis has not been made.

a. Lead

Gold[4] has found four sets of oscillations in lead which he labeled α, β, γ_2, and γ_1 in order of increasing period, or decreasing wave-number cross section. In terms of a picture such as the valence-four picture of Fig. 1, he

TABLE I. Areas of Fermi-surface sections in lead in units of $(2\pi/a)^2=0.45$ atomic unit.

Oscillation type	Assumed band	Single OPW	Experimental[a]
α, (100) field	2nd	1.82	1.11
α, (110) field	2nd	1.04	1.00
β, (100) field	3rd (central hole)	0.13	0.30
γ_2, (110) field	3rd (center arms)	0.16	0.11
γ_1, (110) field	3rd (end of arms)	0.14	0.11

[a] See reference 4.

associated the α oscillations with the second-band surface, the β oscillations with the hole through the center of the horizontal "anchor ring" of the third band, the γ_1 oscillations with the pockets in the fourth band, and the γ_2 oscillations with orbits around the "arms" of the third-band surface. We prefer to make one minor modification in this interpretation and associate both the γ_1 and γ_2 oscillations with orbits around the arms in the third band, the larger-period set being associated with minimum cross sections near the ends of the arms. There are several reasons for suggesting this modification: The variation of the period of the γ oscillations with orientation would indicate that the arms are tapered toward the ends[27] implying that such minima must exist; also, the single-OPW approximation suggests such a taper. Further, Gold has indicated that it would be surprising if the fourth-band pockets were as large in section as the third-band arms since the existence of energy gaps should reduce the fourth-band pockets considerably. In our interpretation we will also find the experimental periods more nearly alike than we expect, but find the discrepancy more in line with modifications expected from the existence of gaps. Either interpretation appears to be consistent with the general orientation dependence, and the agreement with the single-OPW approximation is comparable for the two interpretations.

Table I lists the relevant areas as calculated using the single-OPW approximation and as measured by Gold. It is convenient in interpreting these to note that the area of a square face in the zone is one-half in these units. As was expected, these areas are only in semi-quantiative agreement. The large discrepancy with respect to the area of the second-zone surface perpendicular to a (100) field is to be expected, since the major part of the edge of this area lies along a ridge which will be rounded by the introduction of more OPW's; the edges of all other sections listed at most *cross* ridges. The remaining discrepancies correspond to shrinking of the 3rd-band arms around the symmetry lines as is observed in aluminum and expected upon the basis of the band calculations in the preceding paper.

Gold also obtained effective-mass data from the temperature dependence of the amplitudes of the oscillations. This will be considered in the section on cyclotron resonance which follows.

b. Aluminum

The interpretation of the data in aluminum is discussed extensively in reference 6 and in the preceding paper. We simply repeat the remark that there is a question whether the long-period oscillations (γ_1 in the table) are to be associated with orbits around the ends of the arms or with small regions surrounding lines of contact in the third band. The comparison with the single-OPW calculations is given in Table II. Gold's notation for the oscillation types is used. The agreement may be regarded as somewhat better than that for lead, since the areas in question are much smaller and shortcomings of the model would make much larger percentage errors in the areas; that is, we infer that the matrix elements of the effective potential are somewhat smaller in aluminum.

c. Zinc

We now proceed to zinc and cadmium which have not been previously interpreted with a single-OPW or "nearly-free-electron" approximation. Both metals are hexagonal-close-packed and therefore correspond, except for differences in c/a ratio, to the appropriate pictures in Fig. 3. The available data are more extensive for zinc, and we consider it first.

The most complete de Haas-van Alphen data for zinc have been given by Verkin and Dmitrenko,[28] who observed three sets of oscillations. The most prominent set they attributed to needle-like segments of Fermi surface lying parallel to the c axis. The maximum period observed was 0.62×10^{-4} (gauss)$^{-1}$ corresponding to an area of 0.000154 A^{-2}. We consider these first and seek the corresponding segments in a figure such as Fig. 3. We should first consider how these surfaces change as the c/a ratio is altered. Figure 3 as drawn corresponds to the ideal c/a ratio of 1.6330. As c/a increases, the diagonal arms in the combined first and second bands for valence 2 stretch further and further

TABLE II. Areas of Fermi-surface sections in aluminum in units of $(2\pi/a)^2=0.68$ atomic unit.

Oscillation type	Assumed band	Single OPW	Experimental[a]
γ_2(110) field	3rd (center arms)	0.022	0.011
γ_1(110) field	3rd (end of arms)	0.001	0.001

[a] See reference 5.

[27] The ratio of periods of the γ oscillations for fields in the (100) direction to that for fields in the (110) direction is 0.78, implying a ratio of sections of the surface of 1.3 for the two orientations. If the surface were cylindrical, this ratio would be $\sqrt{2}$; the fact that it is smaller implies a taper toward the ends.

[28] B. I. Verkin and I. M. Dmitrenko, Izvest. Akad. Nauk (S.S.S.R.) Ser. Fiz. **19**, 409 (1955) [translation: Bull. Acad. Sci. (U.S.S.R.) **19**, 365 (1955)].

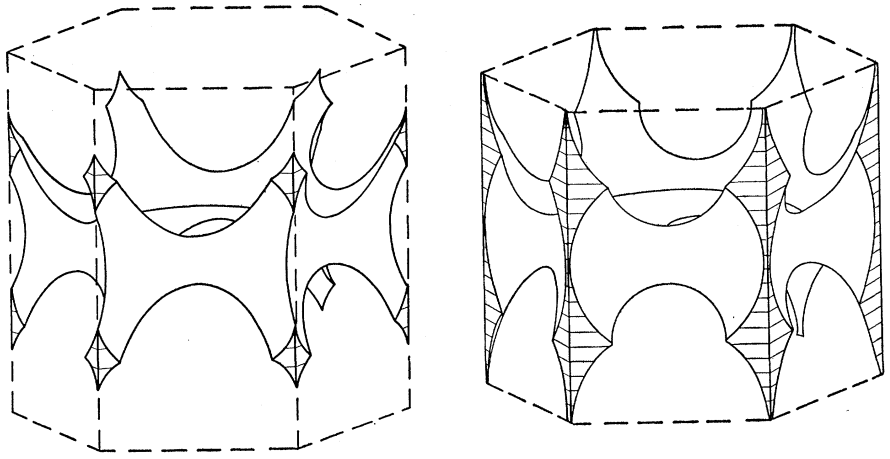

FIG. 4. Fermi surface in the combined first and second bands of divalent hexagonal-close-packed metals according to the single-OPW approximation. The figure on the left corresponds to an ideal c/a ratio of 1.633; that on the right to a c/a ratio of 1.862, roughly that of cadmium.

toward the top and bottom faces of the zone while the ridges near the lateral edges move closer to the edges; at the same time, the needles lying along the edges in the combined third and fourth bands become smaller. At the critical c/a ratio of 1.8607, the arms in the first and second bands reach the horizontal faces, the ridges disappear with the surface meeting the zone faces all along the lateral edges, and the needle-like portions in the third and fourth bands disappear. At c/a ratios above this the first- and second-band surface resembles that shown in the right-hand side of Fig. 4; segments of surface near the zone corners may be rearranged to see that needle-like portions of holes exist at the corners and lie along the c axis. Because the c/a ratio in zinc lies near the critical value, we cannot be certain at first whether the needles seen by the de Haas-van Alphen effect are electrons in the third and fourth bands or holes in the first and second bands.

The cross-sectional area of these segments in the single-OPW approximation may be evaluated and is given approximately by

$$A=\frac{4}{\sqrt{3}}\left(\frac{2\pi}{a}\right)^2\left[\left(\frac{27\sqrt{3}}{8\pi}\frac{a}{c}\frac{z}{2}\right)^{\frac{1}{3}}-1\right]^2, \qquad (8)$$

where z is the valence of the metal; two for zinc and cadmium. The area corresponds to electrons in the third and fourth bands if the expression in the square brackets is positive, and to holes in the first and second bands if it is negative. This may be set equal to the observed area and solved for the necessary c/a ratio; we obtain 1.8419 for electrons, 1.8799 for holes. The true c/a ratios necessary to explain the observed areas would presumably be somewhat farther from the critical ratio of 1.8607 since the effect of the lattice potential would be to reduce the areas in either case.

The observed c/a ratio in zinc is 1.856 at room temperatures, but we note that the de Haas-van Alphen data have been taken at low temperatures. We may estimate the c/a ratio in zinc at low temperatures from the thermal expansion coefficients measured by Grüneisen and Goens[29] in single crystals of zinc. A value of 1.8246 has been obtained in this way. This clearly favors the association of the oscillations with electrons in the third and fourth bands. If we accept this interpretation we may compare the single-OPW estimate with experiment; taking the c/a ratio as 1.8246 at low temperatures, we obtain from (8) an area of 0.00056, four times the area observed experimentally. This agreement may be regarded as good in view of the smallness of segment involved and the uncertainty of the low temperature c/a.

Another aspect of this data which bears on the question as to which segment of the surface is involved is the variation of the period with orientation. We note that the segments of electrons are ellipsoidal, whereas the segments of holes are hyperbolic in shape. We have replotted the data of Verkin and Dmitrenko on the variation of period with orientation in Fig. 5 along with a curve fitted to their data at $\theta=0$ and calculated

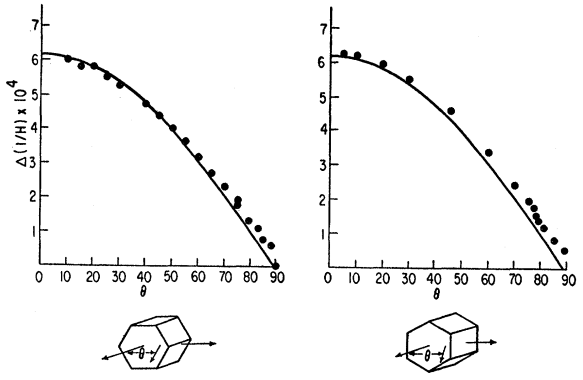

FIG. 5. Experimental variation of the longest-period de Haas-van Alphen oscillations in zinc as observed by Verkin and Dmitrenko (see reference 28). The field orientations are indicated in the figures below. The curves represent the variation of periods for an infinite cylindrical Fermi surface with its axis parallel to the c axis and its cross section adjusted to fit the data for fields parallel to the c axis.

[29] E. Grüneisen and E. Goens, Z. Physik **29**, 141 (1924).

assuming a cylindrical shape. (This curve is simply $0.62\cos\theta$.) The fact that the experimental points lie above this curve for large θ implies that the cross-sectional area is growing more slowly with rotation than it would for a cylinder and therefore that the shape is of the ellipsoidal type. This confirms our supposition that the relevant surfaces are the needle-shaped segments of electrons in the combined third and fourth bands.

There are several other sets of de Haas-van Alphen data which we should consider in the light of this interpretation. These involve the variation of the period with temperature, with alloying, and with pressure; we consider these next.

Berlincourt and Steele[30] have found that the period of the de Haas-van Alphen oscillations in zinc increases rapidly with temperature, rising from 0.064 $(k\,\text{gauss})^{-1}$ at 4.2°K to 0.125 $(k\,\text{gauss})^{-1}$ at 61.2°K. This corresponds to a sharp decrease in the cross-sectional area of the Fermi surface. The temperatures involved are much less than the degeneracy temperature, so we do not expect any observable change in period to come from a change in the Fermi energy with temperature, but we do expect to see effects arising from the change in c/a ratio. Since the c/a ratio is increasing with temperature, we expect segments of electrons to decrease in area while segments of holes would be expected to increase in area; thus the observed temperature dependence also supports the interpretation of the oscillations as arising from electrons. Though the data on the thermal expansion coefficients in this temperature range are scant,[29] we may use it to estimate the change in area according to the single-OPW approximation. We obtain a decrease in this temperature range from 0.00056 to 0.00048 A^{-2}. This is to be compared with the observed change from 0.00015 to 0.00008 A^{-2}.

A change in the period of the oscillations upon alloying with copper has been observed by Marcus,[31] who found that the period decreased due to the addition of copper. He also found an increase in period upon alloying with aluminum, but this increase was within the error of the experiments. These results represent an increase in cross section as the electron density decreases, and interpretation on the basis of the rigid-band model, of course, would indicate that holes are involved. Such an interpretation overlooks the change in c/a ratio which occurs with alloying. It is seen from Eq. (8) that the cross section of the segments of Fermi surface in question depend upon za/c, rather than simply z. Consider first the addition of copper to zinc; Owen and Pickup[32] have found that the addition of 1.85 atomic-percent copper to zinc lowers the c/a ratio from 1.856 to 1.817 and that the changes were linear in concentration; thus the addition of 1.85 atomic-percent copper raises za/c from 1.078 to 1.091. Hence the inclusion of the effects of the c/a ratio just reverses the direction of the effect and an increase in area with addition of copper actually supports our proposal of electrons rather than holes. Owen and Imball[33] find that the addition of 3 to 5 atomic-percent aluminum raises the c/a ratio to 1.869, thus za/c is raised to 1.086 or 1.096. This should give a shift in the de Haas-van Alphen period of opposite sign to that suggested by Marcus, but neither the de Haas-van Alphen nor the x-ray data were conclusive for this case, so we do not give the result much weight.

Quite recently a change in the de Haas-van Alphen period with pressure was observed by Dmitrenko, Verkin, and Lazarev,[34] and their observations appear to be in contradiction with our proposal. They found that increased pressure gave increased period and therefore *decreased* area. Furthermore, they note that the c/a ratio becomes more nearly ideal as the pressure is increased so we should expect the area of the electronic sections to *increase*. One might suggest the possibility that the applied pressure was not isotropic, in which case this experiment would not be meaningful. However, still more recent studies by Verkin and Dmitrenko[35] of the change in de Haas-van Alphen period with uniaxial compression and tension along the c axis, confirm their conclusion that a reduction of the c/a ratio reduces the cross section of the segments of Fermi surface in question. This one effect does not agree with our proposed interpretation and is somewhat disturbing. We note, however, that these changes in period are small (of the order of a few percent) and are accompanied by very large and unexplained reductions in amplitude. The weight of the evidence seems to support our proposal; this one effect remains anomalous.

We will now consider the other sets of oscillations observed in zinc by Verkin and Dmitrenko.[28] Their data representing these other sets are plotted in Fig. 6. Consider first the smallest periods observed. These correspond to an area of 0.048 A^{-2}. We should expect them to be associated either with the horizontal or with the diagonal arms shown in Fig. 4. The single-OPW areas of these are 0.045 and 0.06 A^{-2}, respectively. The fact that they are relatively independent of orientation in the range in which they are observed is inconsistent with the expected orientation dependence for the horizontal arms, so we associate them with the diagonal arms. The curves shown are calculated for these arms assuming a cylindrical cross section, oriented appro-

[30] T. G. Berlincourt and M. C. Steele, Phys. Rev. **95**, 1421 (1954).
[31] J. Marcus, Phys. Rev. **77**, 750 (1950).
[32] E. A. Owen and L. Pickup, Proc. Roy. Soc. (London) **A140**, 179 (1933).
[33] E. A. Owen and J. Imball, Phil. Mag. **17**, 433 (1934).
[34] I. M. Dmitrenko, B. I. Verkin, and B. G. Lazarev, J. Exptl. Theoret. Phys. (U.S.S.R.) **33**, 287 (1957) [translation: Soviet Phys.—JETP **6**, 223 (1958)].
[35] B. I. Verkin and I. M. Dmitrenko, J. Exptl. Theoret. Phys. (U.S.S.R.) **35**, 291 (1958) [translation: Soviet Phys.—JETP **8**, 200 (1959)].

priately. These curves correspond to a cross section of 0.048 A^{-2}, in suitable agreement with our single-OPW value of 0.06.

The intermediate-period oscillations have an orientation dependence appropriate to the horizontal arms of Fig. 4, but the corresponding cross-sectional area is 0.00435 A^{-2}, a factor of ten smaller than our single-OPW estimate. The dashed curves shown in Fig. 6 correspond to cylindrical surfaces of the proper orientation. The fact that the data fall below the line at small θ indicates a hyperbolic shape as expected if these are to be associated with the arms of Fig. 4. The lower dashed curve on the left is not expected to appear, since it has just half the period of the upper curve and would appear in the data only in a change in the shape of the oscillations. Since these, in turn are superimposed upon the longest period oscillations, such a distortion cannot be discerned in the data. Because of this very good fit to the orientation dependence, and because we see no other segments which would fit the data, we must conclude that their oscillations are to be associated with the horizontal arms of Fig. 4.

The fact that the observed arms are very much smaller than calculated in the single-OPW approximation implies that a matrix element connecting a pair of the OPW's in this region must be large. Furthermore, this must be the matrix element associated with the reciprocal-lattice vector parallel to the c axis or the diagonal arms would be similarly distorted. It does not seem surprising that this Fourier component of the potential is larger than the others; in fact, if we examine the beryllium band calculation (beryllium is also divalent and hexagonal-close-packed) by Herring and Hill[36] we note that they find a large band gap associated with this lattice vector as evidenced by the 5 electron-volt splitting between Γ_3^+ and Γ_4^-. This is perhaps easier to see in the comparison of the band calculation and the "empty-lattice approximation" as given by Herman.[37]

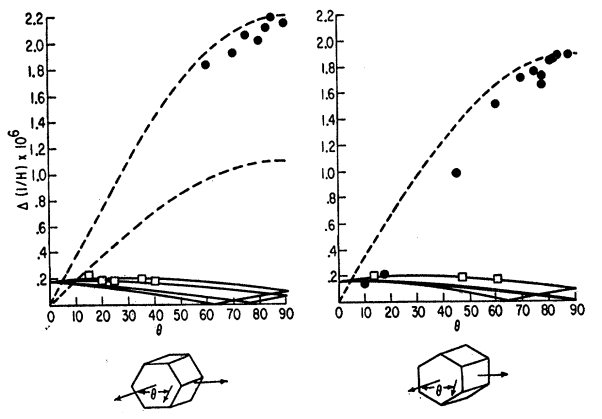

FIG. 6. Experimental variation with orientation of the short-period de Haas-van Alphen oscillations in zinc as observed by Verkin and Dmitrenko (see reference 28). The field orientations are indicated in the figures below. The dashed curves represent the variation of periods for infinite cylindrical segments of Fermi surfaces with axes parallel to the edges of the hexagonal faces and with cross sections adjusted to fit the data for fields along such an edge. The solid curves represent the variation of periods for infinite cylindrical segments of Fermi surface with axes given by $\theta=\arctan(a/c)$ in the figure on the left. The maximum period was adjusted to fit the data for fields along the cylinder axis.

This is the first case we have encountered where there is a very large distortion of the single-OPW surfaces by the lattice potential. Even in this case it is possible to isolate the region of surface giving rise to each set of oscillations.

We should also note the implications of this large band gap for the horizontal disk in the combined third and fourth bands. The minimum cross-sectional area of this surface is 0.7 in the single-OPW approximation. We may expect this segment to be drastically reduced in area by the distortion associated with this gap. Even though the area of this segment may be greatly reduced, we could not associate it with the smallest-period oscillations observed because of the orientation dependence. Furthermore, we would expect its associated period to be smaller than the smallest period observed.

Finally, the V-shaped segments of electrons in the combined third and fourth bands should not be distorted appreciably; the large band gap does not affect them. Their cross-sectional area is comparable to that of the horizontal disk and their period significantly smaller than the smallest period observed. Thus oscillations have been observed for the three smallest sections of the surface; the largest sections remain unseen.

d. Cadmium

The picture in cadmium is somewhat simpler. The c/a ratio at room temperature is 1.884, and corrected to low temperatures using the thermal expansion data of Grüneisen and Goens[29] it becomes 1.862. This is well within error of the critical ratio 1.8607 at which the regions of holes along the lateral zone edges vanish, as well as the regions of electrons along these edges. Thus it is not surprising that oscillations corresponding to the lowest frequency oscillations in zinc have not been observed in cadmium. It should be noted that since the lattice potential tends to reduce the cross sections of any such segments, both will fail to appear over a range of values of c/a near 1.8607.

The diagonal arms in the first and second bands are expected to give rise to oscillations, however, and their orientation and minimum area may be evaluated assuming a c/a ratio of 1.862. We find that they are expected to lie 28.23° from the c axis [$\text{arc cot}(c/a)=28.23°$], and have a minimum cross-sectional area of 0.054 A^{-2}, the latter being obtained graphically. Berlincourt[38] has found segments of Fermi surface lying 28.5° from the c axis and having a maximum

[36] C. Herring and A. G. Hill, Phys. Rev. **58**, 132 (1940).
[37] F. Herman, Revs. Modern Phys. **30**, 102 (1958).
[38] T. G. Berlincourt, Phys. Rev. **94**, 1172 (1954).

period of 1.88×10^{-7} (gauss)$^{-1}$, corresponding to a minimum area of 0.051 A^{-2}. This close quantitative agreement of the single-OPW approximation with experiment should probably be regarded as fortuitous.

We might also expect oscillations arising from the horizontal arms in the first and second bands, corresponding to the intermediate oscillations in zinc, but these have not been observed. The single-OPW section is 0.037 A^{-2}, even smaller than the corresponding section in zinc and significantly smaller than the diagonal arms in cadmium which have been observed. Thus it seems plausible to say that the distortion in this region is even larger than it is in zinc and, in particular, that it is large enough to pinch off these arms completely and isolate the sections near the lateral zone edges. Presumably the larger sections in the third and fourth bands are present as in zinc.

In addition to these four metals, de Haas-van Alphen oscillations have been observed in thallium, which is close-packed hexagonal and valence 3. From Fig. 3 it is seen that there are several possible sources of oscillations in this metal, and it is not clear which set is causing the observed oscillations. Although no oscillations have been reported in calcium or strontium, they would appear promising; both are face-centered cubic and divalent. The very thin sections indicated in the appropriate first-band figure of Fig. 1 would be expected to vanish under the influence of the lattice potential yielding arms lying along (110) directions. Barium would also look promising; it is body-centered cubic and divalent. The arms lying in (111) directions and indicated in Fig. 2 would seem ideal for de Haas-van Alphen study. Some data exist for several other metals of the types discussed here but are insufficiently complete to warrant a comparison with theory. Finally, extensive data exist on tin and on the semimetals, but these are outside the realm of metals considered here, though they may very well be appropriate for single-OPW study. This approach could be regarded as only a preliminary step in the semimetals. Bismuth, for example, is pentavalent and has two atoms per cell so that the appropriate single-OPW sphere contains ten electrons. Segments of the surface lie in bands two through eight, and are in all cases fairly small. Presumably all of these segments collapse except for segments surrounding holes in the fifth band and electrons in the sixth. The consideration of the potential required to clarify the picture is more detailed than is appropriate here.

2. Cyclotron Resonance

As has been indicated, the cyclotron-resonance experiments measure a frequency of the electron orbits. In the customary picture of cyclotron resonance in metals, the electron orbits lie largely in the body of the material where the applied high-frequency fields do not penetrate; it is only small portions of the orbits which lie within the skin depth, so if the applied fields are properly synchronized with the orbit frequency, an electron will see a field in the same direction each time it traverses this segment of the orbit, thus giving a resonant effect. Now electrons in the presence of a magnetic field move in helical orbits with the helical axis lying along the magnetic field. Thus most electrons will have a net drift along the field. Experimentally, one applies the field parallel to the surface so that this drift would not take the electrons away from the region of the surface; thus any collection of electrons could give an observable effect as long as a large enough number of electrons with nearly the same frequency is involved. Phillips,[39] however, has suggested that the field is never aligned sufficiently well for this to be the case and that any electrons which drift along the field will quickly drift into the surface or out of the skin depth and will not contribute to the resonance. If this is the case, an additional condition for observable resonance is the existence of a vanishing drift velocity.

It can readily be shown that this condition is equivalent to that for the observation of de Haas-van Alphen oscillations; i.e., that the cross-sectional area be extremal at the point in question. To see this we let the field lie in the z direction, and draw the intersection of a plane, $k_z=$constant, and the Fermi surface. This intersection represents the orbit of an electron in wave-number space. We also project on this plane the intersection of the Fermi surface and a neighboring plane, displaced by δk_z from the first plane. These intersections are drawn schematically in Fig. 7. We may evaluate the energy associated with a point on the projected intersection to first order in the quantity δk_z and set it equal to zero, since both intersections lie on the Fermi surface;

$$\delta E=(\partial E/\partial k_z)\delta k_z+(\partial E/\partial k_\perp)\delta k_\perp+(\partial E/\partial k_{11})\delta k_{11}=0.$$

We note that $\partial E/\partial k_{11}=0$, so the above equation gives

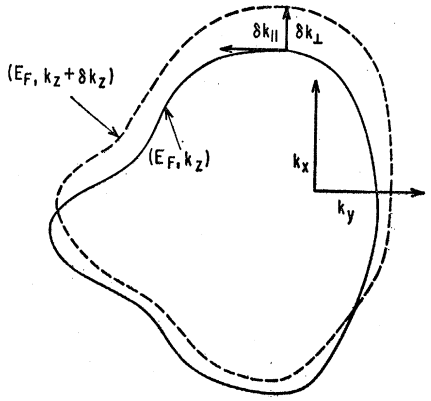

FIG. 7. The projection of two neighboring electronic orbits in wave number space onto a plane perpendicular to the magnetic field. Both orbits correspond to electrons with the Fermi energy. The magnetic field lies along the k_z axis.

[39] J. C. Phillips, Phys. Rev. Letters 3, 327 (1959).

us a relation between $\delta k_\perp$ and δk_z. We may take a time integral of the equation around the orbit, replacing the derivatives of energy with respect to wave number by the appropriate electron velocities, and using (3) to eliminate the component of velocity perpendicular to the field. We obtain

$$\hbar\delta k_z \oint v_z dt + (\hbar^2 c/eH) \oint \delta k_\perp \dot{k} dt = 0.$$

The first term is equal to $2\pi\hbar\delta k_z \bar{v}_z/\omega_c$, where $\bar{v}_z$ is the drift velocity along the field. The cyclotron mass $m^* = eH/c\omega_c$ is introduced and we solve for $\bar{v}_z$,

$$\bar{v}_z = \frac{\hbar}{2\pi m^*} \frac{\partial A}{\partial k_z}, \tag{9}$$

where A is the orbit area in wave-number space. Thus the condition that the drift velocity vanish is equivalent to the condition that the cross-sectional area be extremal.

Phillips has indicated that under typical conditions for cyclotron resonance, tilting the field by even half a degree to the surface restricts the electrons which contribute to the surface conductivity to those with very small drift velocity. One might argue that irregularities of the surface will guarantee such misalignments, but it should be noted that because of surface irregularities there will be *some* regions of the surface which will be very closely aligned with the field. It is conceivable that the observed absorption arises largely from such regions; this also would explain the occurrence of resonances when the field is tipped slightly out of the apparent surface of the specimen. For fields exactly parallel to the surface, an observable resonance may occur whenever there is a sufficiently sharp peak in the distribution of masses.

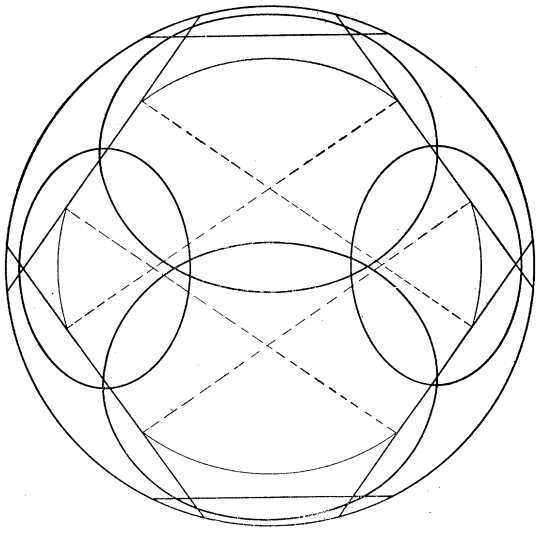

FIG. 8. The Fermi sphere in aluminum, and its intersections with Bragg-reflection planes, projected on a (110) plane. One particular electron orbit corresponding to a magnetic field in the (110) direction is illustrated; the dashed portions indicate Bragg reflections.

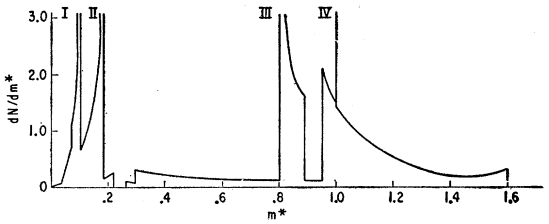

FIG. 9. The distribution of cyclotron masses in aluminum according to the single-OPW approximation for a magnetic field in the (110) direction. A free-electron energy dependence was assumed. The curve is normalized such that $\int (dN/dm^*) dm^* = 1$. The numbered peaks correspond to extremal orbits discussed in the text.

Thus there remains an uncertainty as to whether the condition of extremal area is necessary for observation of a resonance. Coupled with the fact that sometimes a particular resonance may not appear for other reasons, (as is suggested by zinc data to be discussed) this leaves a considerable ambiguity in the interpretation of cyclotron-resonance data unless the data include sufficient orientation dependence to isolate the section of Fermi surface in question.

In spite of this difficulty, we may frequently make a reasonable interpretation of the data in terms of the single-OPW surfaces. We will illustrate this by selecting a particular orientation of the magnetic field for a particular metal and determining the distribution of cyclotron masses. We give a detailed treatment of aluminum, followed by more cursory treatments of other metals for which suitable data exist.

a. Aluminum

We let the field lie in the (110) direction. The reduced-zone representation used for the de Haas-van Alphen effect was found inconvenient for treatment of cyclotron resonance because of the difficulty in determining the velocity of the orbit in wave-number space over the various portions of the surface. It is more convenient to construct the Fermi sphere with its intersections with Bragg planes. This figure, then, is projected onto a (110) plane for a field in the (110) direction as shown in Fig. 8. The projection of the electron wave number then moves with constant angular velocity in this figure under the influence of a constant field, making discontinuous jumps when the orbit intersects the projection of an intersection of the sphere with a Bragg-reflection plane. One such orbit is sketched in the figure, with dashed lines indicating the Bragg reflection. To determine the period of the orbit, one simply adds the total angle through which the orbit moves (not counting the Bragg reflections), and this is proportional to the period. It is easily seen that the particular orbit drawn in Fig. 8 has a period less than the corresponding orbit in the absence of Bragg

TABLE III. Cyclotron masses in aluminum in units of the electronic mass.

1 OPW mass-one	Experimental Langenberg and Moore[a]	Fawcett[b]	Gunnersen[c]
I 0.10	0.18±50%	0.11	0.15
II 0.17	0.18±50%	0.23_5, 0.21_5	
III 0.80	1.5 ±10%		

[a] D. N. Langenberg and T. W. Moore, Phys. Rev. Letters 3, 137 (1959).
[b] E. Fawcett, Phys. Rev. Letters 3, 139 (1959).
[c] See reference 5.

reflections. Taking the effective mass associated with the sphere without reflections as unity, the distribution of cyclotron masses has been evaluated and is shown in Fig. 9. It is seen that there exist masses over almost all of the range zero to 1.6. Extremal masses are represented by the singularities I, II, III, and IV corresponding to orbits around the third-band arms lying parallel to the field, third-band arms lying at an angle to the field, central orbits around the second-band surface, and circular orbits on the surface of the third-band arms, respectively. (The orbits IV lie at the center of Fig. 8.) The orbits I and III correspond also to extremal *areas* and orbit II very nearly does. These, therefore, have vanishing, or very nearly vanishing, drift velocities and should be observable even if the conjecture of Phillips is correct. Orbits IV have large drift velocity; furthermore, they involve such a small number of electrons and are sufficiently sensitive to distortions arising from the lattice potential, that they might not be observable in either case. The peak at $m^*=1.6$ corresponds to a maximum mass and a maximum area, but these maxima are sharp in the single-OPW approximation and will remain fairly sharp in a more complete calculation so that the number of electrons involved may be expected to be quite small compared to that of the peak III. Though it would be tempting to associate this peak with the observed high mass of 1.5, it seems unlikely that resonances associated with this peak should appear and those with peak III not. Thus we expect the peaks I, II, and III to give the most prominent resonances, and we associate these with the observed resonances. It may be noted that these are just the peaks we would most naturally select by examining the surfaces of Fig. 1, so we will use the reduced-zone figures to select the relevant segments in interpretating the other metals, in each case determining the actual masses graphically.

The appropriate masses for fields along a (110) axis in aluminum were determined from Fig. 9 and are listed in Table III. It may be noted that the values differ from those given in the preceding paper by a factor of 1/0.79 because we have used a mass-one parabola rather than that determined from the band calculation. The corrections listed with Langenberg and Moore's results reflect the anisotropy of the mass which they observed and the fact that the numbers they give did not correspond to fields along the (110) direction. Their measurements and those of Fawcett were determined from cyclotron-resonance measurements; those of Gunnersen are based on the temperature dependence of the de Haas-van Alphen amplitudes. The agreement is semiquantitative; the most disturbing comparison is that of III, where the influence of the lattice potential should be smallest and our agreement the best. The fact that we tend to underestimate the mass has been discussed in the preceding paper.

b. Lead

Cyclotron resonance has apparently not been observed in lead directly, but Gold[4] made mass determinations for various segments of the Fermi surface from the temperature dependence of the de Haas-van Alphen oscillations. Because they are directly associated with the de Haas-van Alphen oscillations, there is no ambiguity in their interpretation except for the ambiguity we have mentioned in the interpretation of the periods. The masses as determined by Gold are listed in Table IV, along with the masses determined from the single-OPW approximation. We notice that the agreement with experiment is very much improved by doubling all of the calculated masses, as was the case in aluminum. The β oscillations show an experimental mass which is considerably higher than we expect, even if we make the factor-of-two correction. The doubling of the masses is consistent, as in aluminum, with the experimental electronic specific heat,[40] which is approximately twice the free-electron value.

c. Zinc

Cyclotron resonance has been observed in zinc by Galt, Merritt, Yager, and Dail.[41] With a field along the six-fold axis they find evidence for a carrier with mass less than 0.015, presumably corresponding to the mass of 0.0068 obtained from the de Haas-van Alphen effect (this is the geometric mean, $(m_1m_2)^{\frac{1}{2}}$, of the masses given by Shoenberg[42]). In addition, they find a mass of

TABLE IV. Cyclotron masses in lead in units of the electronic mass.

Oscillation type	Assumed band	Single OPW (mass one)	Experimental[a]
α, (100) field	2nd	0.95	
α, (110) field	2nd	0.57	1.0 ±0.1
β, (100) field	3rd (central hole)	0.17	1.33±0.15
γ_2, (110) field	3rd (center arms)	0.22	0.56±0.06
γ_1, (110) field	3rd (end of arms)	0.19	0.56±0.06

[a] See reference 4.

[40] R. L. Dolecek, Phys. Rev. **94**, 540 (1954).
[41] J. K. Galt, F. R. Merritt, W. A. Yager, and H. W. Dail, Jr., Phys. Rev. Letters **2**, 292 (1959).
[42] D. Shoenberg, *Progress in Low Temperature Physics* (Interscience Publishers, Inc., New York, 1959), Vol. II, p. 226.

0.55 ± 0.03 for this field orientation and tentative evidence that the latter arises from electrons rather than holes. Finally, they find a mass of 0.43 ± 0.04 for fields along a binary axis and indications that it also arises from electrons. If it is true that the heavy-mass resonances are associated with electrons, they must arise either from segments in the 3rd and 4th bands or, when the field is parallel to the c axis, from orbits around the central hole in the 1st and 2nd bands. This suggestion is supported by the fact that the masses associated with the segments observed in the de Haas-van Alphen effect would be expected to be smaller than those observed by a factor of at least four, whereas the mass calculated for the central disk in the 3rd and 4th bands, for example, ranges from 0.39 to 1.00 in the single-OPW approximation. In the absence of orientation dependence of these masses, it would seem a little bold to associate them with particular segments of the surface.

The low-mass carriers, on the other hand, certainly correspond to the needle-shaped segments which we have discussed. In the single-OPW approximation, these have a cyclotron mass for fields parallel to the c axis of 0.011 assuming a mass-one single-OPW parabola and a c/a ratio of 1.8246. If we were to assume a slightly different c/a ratio of 1.8425, which would bring the observed *area* into agreement with experiment, we obtain a mass of 0.005, to be compared with the experimental value of 0.007 obtained by Shoenberg. The agreement with experiment is remarkable in either case in view of the smallness of the segment and its sensitivity to the c/a ratio.

d. Cadmium

Cyclotron resonance has not been observed directly in cadmium, but Berlincourt[38] made an estimate of the cyclotron mass from the temperature dependence of the de Haas-van Alphen amplitudes. He obtained a value of 0.141 for fields parallel to the diagonal segment in the combined first and second bands. This is to be compared with the single-OPW value of 0.142, obtained using a c/a ratio of 1.862. As was the case in considering the cross-sectional areas of these arms, the agreement is too close to be regarded as other than fortuitous. We can note, however, that the factor-of-two discrepancy found in lead and aluminum does not appear in cadmium.

There is insufficient data for other metals encompassed by our analysis here to warrant further comparisons with experiment.

3. The Anomalous Skin Effect

Since only the curvature of the Fermi surface affects the anomalous surface resistance and since it enters in such a way that regions of very large curvature do not enter, the change in the connectivity of the Fermi sphere in the single-OPW approximation does not affect the results. Thus in the single-OPW approximation the surface impedance is, strictly speaking, isotropic and determined only by the number of conduction electrons present. On the other hand, we will be able to see how the introduction of the lattice potential will affect the orientation dependence of the surface impedance by examination of the single-OPW approximation, and this seems appropriate for consideration here. As an example, we will treat aluminum with some care.

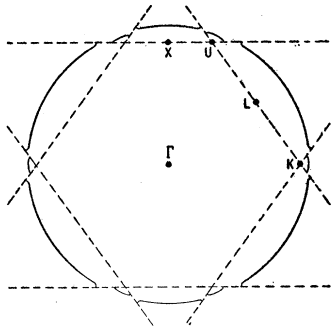

FIG. 10. The Fermi surface in aluminum in the extended-zone scheme according to the multiple-OPW calculation of the preceding paper. Shown is the intersection of the Fermi surface with a central (110) plane. The dashed lines represent Bragg-reflection planes.

It is most convenient to treat this effect in the extended zone scheme, as we did the cyclotron resonance. A central (110) cross section of the Fermi surface was determined from the band calculation of the preceding paper and is shown here in Fig. 10. It is seen that the Fermi surface is sheared wherever it intersects a Bragg-reflection plane. The main effect, as far as the anomalous skin effect is concerned, may be the opening up of gaps in the sphere at these intersections. Thus, as a starting approximation, we treat the Fermi surface as a sphere with gaps opened up at each intersection with a Bragg plane; such intersections have been shown for aluminum in Fig. 8. Such a figure will, in fact, be very convenient for treating the anomalous skin effect graphically.

A formula for the surface impedance in the extreme anomalous limit has been given in Eq. (6),

$$R_x=\frac{\sqrt{3}}{2}\left(\frac{\pi\omega^2h^3}{e^2\int|r_y|\,dk_y}\right)^{\frac{1}{3}}.$$

For a spherical Fermi surface, the points where the intersection of the Fermi surface and a plane $k_y=$constant is parallel to the z direction lie in the x-y plane. Thus the integration is taken over the intersection of the Fermi surface and the x-y plane. For a spherical Fermi surface, the integral $\int|r_y|\,dk_y=\pi k_F^2$. For a sphere with gaps we must subtract off the integration over the gaps. In the spirit of the single-OPW approximation we regard the gaps as small and obtain

$$R_x=R_x^0\left[1+(1/3\pi k_F^2)\int_{\text{gaps}}|r_y|\,dk_y\right],$$

R_x^0 being the surface impedance for the complete

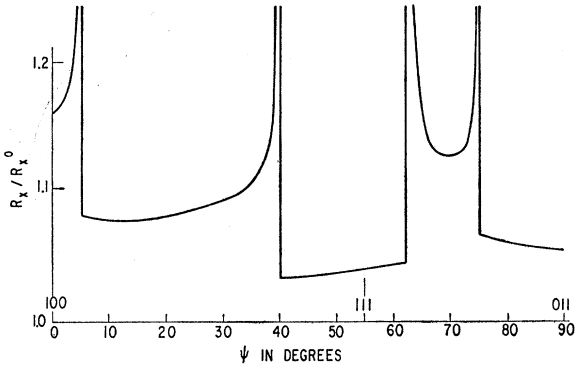

FIG. 11. The calculated surface impedance of aluminum as a function of the surface orientation. R_x^0 is the surface impedance of a three-electron sphere; R_x is the surface impedance of a three-electron sphere with suitable gaps introduced at the Bragg-reflection planes. The normal to the surface lies in a $(01\bar{1})$ plane and makes an angle ψ with the (100) direction; R_x is the surface impedance in the $(01\bar{1})$ plane.

spherical surface. Now let the gap lying along a particular Bragg-reflection plane have a small width, Δ. Then the region of the integration at each intersection of a gap with the x-y plane is $dk_y=(\Delta/k_F)(|r_y|/|\sin\theta|)$ where θ is the angle between the line of the gap and the x-y plane. The integration over the gaps becomes a summation over the intersections of the gaps and the x-y plane and we obtain

$$R_x=R_x^0\left(1+\frac{1}{3\pi}\sum_{\text{gap int}}\frac{r_y^2}{k_F^2}\frac{\Delta}{k_F}\frac{1}{|\sin\theta|}\right).$$

If we wish to proceed graphically from Fig. 8, it is convenient to write $r_y^2=k_x^2$ and note that $1/\sin\theta=[1+\cot^2\theta'/(1-k_x^2/k_F^2)]^{\frac{1}{2}}$, where θ' is the angle of intersection of the x axis and the *projection* of the Bragg-reflection line onto the x-z plane. Then the axes are taken with y perpendicular to the plane of Fig. 8, and all relevant quantities may be measured directly from the figure. This procedure has been followed in order to find the surface impedance for the normal to the surface lying in directions ranging from a (100) direction to a (011) direction. For this calculation Δ/k_F was estimated from Fig. 10 to be 0.05 for gaps associated with intersections of the sphere and a (111) plane, and 0.10 for gaps associated with intersections with a (200) plane. The resulting curve is shown in Fig. 11. The graphical scheme used becomes somewhat inaccurate in the region of the peaks, but the sharpness of the peaks, in any case, comes from treating the gaps as very narrow and a great deal of smoothing would be expected from a better calculation.

It is difficult to assess the reliability of this somewhat crude approximation and, unfortunately, there apparently do not exist data on single crystals of aluminum which would allow us to see if this gives us the main features of the effect. There is a possibility that there may be appreciable distortion of the surface adjacent to the gap which could give large effects; it is not clear that we have isolated the most important source of anisotropy in the surface impedance. Further application of the scheme does not seem warranted until suitable data are taken.

IV. EXPERIMENTAL DETERMINATION OF BAND STRUCTURE

We indicated in the introduction that the single-OPW approximation may be regarded as the zeroth-order approximation in a series of successive approximations for calculating the band structure; the zeroth-order approximation has turned out to provide a reliable semiquantitative theory of the polyvalent metals. This immediately suggests the possibility of using the experimentally-observed deviations from the single-OPW picture in order to improve the approximation to the band structure. The most promising approach would appear to be the use of experimentally-determined sections of the Fermi surface to evaluate the matrix elements connecting particular pairs of plane waves. Once these are obtained, constant energy curves are readily obtained in the manner described in the preceding paper on the band structure of aluminum.

Aluminum itself would appear to be a difficult case to treat in this way; the matrix elements are small, and a careful determination of the Fermi-energy (i.e., the Fermi radius) would be needed at each step in the calculation. Furthermore, the de Haas-van Alphen data are limited.

Lead and zinc, on the other hand, would seem quite suitable for such a treatment. In both cases there is one measured area which is modified appreciably by the presence of a particular matrix element; presumably these elements could be determined neglecting the shift in the Fermi energy. The remaining elements could then be adjusted to fit the remaining measured segments. In both cases there exist enough data to determine the necessary parameters. Again there is the difficulty that a shift in the Fermi energy must be calculated in order that the correct number of conduction electrons are included within the surface; if the Fermi energy were sufficiently sensitive to uncertain details of the surface, it might be preferable to regard it also as an adjustable parameter.

The determination of the parameters in this way leaves an energy scale factor undetermined. One would like to adjust this to fit cyclotron-resonance masses, but the experience with the masses studied in Sec. III of this paper would raise some question as to the meaning of this.

In any case, the band structure determined in this way could be readily compared with a full band calculation from which one obtains the splitting of levels at symmetry points directly, thus bridging the gap between experiments which see the Fermi surface and

calculations which see only symmetry points in the Brillouin zone.

V. ALLOYS

We wish only to make a cursory treatment of alloys. If we consider substitutional alloys and neglect any effects of *local* lattice distortion, we may proceed as in a pure metal. As starting states we take plane waves orthogonalized to the core states (different core states in the regions of different cores). We may then evaluate the diagonal elements $T(\mathbf{k})$ of the Hamiltonian in this representation. If the cores do not overlap, $T(\mathbf{k})$ will be spherically symmetric and will be the weighted average of the $T(\mathbf{k})$ for the constituent metals, each taken for the lattice structure appropriate to the alloy. We again make a Fourier expansion of the pseudopotential and now obtain two types of terms: first, those associated with reciprocal lattice vectors; and second, those which arise from deviations from the periodicity and which may occur for arbitrary wave number. The former are the weighted average of the corresponding Fourier components in the constituent metals. Thus, before we introduce the components of arbitrary wave number, we have a well-defined "average band structure" for the alloy, and we may expect it to describe the alloy in the same sense that the ideal band structure of a metal describes a pure metal at finite temperature. This is the point of view which we took in Sec. III when discussing the alloys of zinc, and is the point of view which seems appropriate when discussing macroscopic properties such as the de Haas-van Alphen effect. If the constituent metals of the alloy may be approximated with a single-OPW approximation, we may also treat the alloy with a single-OPW approximation.

Finally we must consider the effects of the deviations from periodicity. This part of the problem must be done self-consistently since the simple pseudopotential envisaged above may tend to redistribute the conduction electrons in the alloy giving rise to screening fields. These nonperiodic terms will cause scattering between the average-band states and a consequent life-time broadening of the levels. For most problems it would seem more appropriate to include this as a scattering effect rather than as a "fuzzing" or broadening of the bands. In addition to causing scattering, the nonperiodic terms will redistribute the electrons to the regions of particular atomic sites. Although it is plausible to assume that an electron undergoing a helical orbit in magnetic field will behave according to an average band structure, a particular nucleus being observed in a Knight-shift experiment will see a local electronic structure which may differ significantly from the average band structure. Such difficulties are out of the realm of the problems under consideration here and must be studied individually for each problem for which a redistribution of the electrons is of consequence.

VI. CONCLUSIONS

The single-OPW approximation is defined to be the result of an orthogonalized-plane-wave calculation in the limiting case as the matrix elements between individual orthogonalized plane waves become small. It should be emphasized that such an approximation provides a strictly geometrical theory; the energetics of the bands enter only as a scale factor in the various effective mass determinations. Some justification of such a model is made, but it is insufficient to allow us to know just how large our errors will be in a particular metal. Comparison with the results of a band calculation for aluminum in the preceding paper have indicated that it is sufficiently good in that case to give a complete qualitative picture of the Fermi surface and semiquantitative estimates of the parameters which enter many of the electronic properties. The primary purpose of the present work was to determine as well as possible experimentally the applicability of the scheme to polyvalent metals in general.

To this purpose the method was applied to a series of polyvalent metals and compared in some detail with the de Haas-van Alphen data in lead, aluminum, zinc, and cadmium; these being the only metals in the series treated for which sufficient data exist to allow a comparison. In addition, comparison was made with observed cyclotron and specific-heat masses where possible. The apparent validity of the description provided by the simple approach is remarkable in these cases, particularly since the features of the structure which are seen by these effects are the fine details. In the single-OPW approximation, the dimensions of the small segments of the Fermi surface are the differences between nearly equal large numbers; thus this comparison may be regarded as a very sensitive test of the method for these metals. The agreement is particularly close with respect to the areas of segments of the Fermi surface, but is semiquantitative with respect to cyclotron masses as determined either from the de Haas-van Alphen effect or directly (which is remarkable in itself). Even in a particular section of the Fermi surface in zinc for which there appears to be a marked deviation from single-OPW behavior, there was no ambiguity in the interpretation of the de Haas-van Alphen data.

We conclude that the single-OPW approximation provides a good semiquantitative theory of the electronic structure of the polyvalent metals for which an experimental check has been made. Such a method is extremely useful for studying metals. Not only is the application of the method simple, but it requires no knowledge of the metal in question other than its crystal structure and its valence. The Fermi surface constructed in this way provides a simple picture of the electronic structure and one that makes it easy to isolate the features of the surface relevant to particular phenomena and provides a rather reliable framework upon which to base an interpretation of experimental

studies. It also allows at least semiquantitative estimates of the parameters which enter many electronic properties. Finally, it provides a basis for experimentally determining a more precise band structure in terms of the observed deviations from single-OPW behavior. In this last regard, it is worth remarking that for most purposes one does *not* desire a precise description of the band structure. One more generally wishes to have a parameterized model of the structure which is simple enough to allow the calculation of a particular property, but reliable enough to include the important features of that effect.

In connection with the detailed studies of zinc and cadmium, rather explicit descriptions of the Fermi surfaces of these metals emerged. The surfaces resemble those shown in Fig. 3 for valence two. The surfaces in the combined first and second bands are distorted qualitatively in the manner indicated on the right-hand side of Fig. 4, but not to the extent that the lateral ridges on the surface meet the lateral edges of the zone. The ridges are everywhere rounded off somewhat such that the cross sections of the diagonal arms are reduced by a few percent. In zinc the cross section of the horizontal ring is narrowed down by a factor of ten midway between the lateral edges of the zone; in cadmium the ring is pinched off completely in these regions. In the combined third and fourth bands the needle-like segments along the lateral edges of the zone are narrowed down greatly in zinc and disappear in cadmium. In both cases the horizontal central disk is reduced appreciably in size, while the V-shaped segments at the lateral zone faces are rounded off, but presumably not greatly reduced in size.

In addition to the applications mentioned above, a study of the anomalous skin effect in aluminum was made, although there were no suitable data on single-crystal specimens to allow for comparison. The oscillatory magnetoacoustic effect was also discussed briefly in terms of the method. Finally, the generalization of the scheme to a study of alloys was outlined.

PHYSICAL REVIEW VOLUME 118, NUMBER 5 JUNE 1, 1960

Surface Magnetostatic Modes and Surface Spin Waves

J. R. ESHBACH AND R. W. DAMON
General Electric Research Laboratory, Schenectady, New York

(Received January 6, 1960)

Examination of the spatial configuration of the magnetostatic modes of a ferromagnetic body shows that those modes whose frequency lies between $\omega=\gamma(B_iH_i)^{\frac{1}{2}}$ and $\omega=\gamma(H_i+2\pi M)$ are surface modes. It is also found that the complete spin-wave spectrum consists of a set of surface spin waves in addition to the spin-wave band usually considered. The magnetostatic mode spectrum thus merges smoothly into the spin-wave spectrum.

The characteristic equation for the surface modes on a plane surface at an arbitrary angle to the applied dc field is given. The properties of the surface modes on plane surfaces and on spheroidal bodies are discussed.

THE characteristic magnetostatic modes of a ferromagnetic slab, magnetized parallel to its surface, were recently examined by the authors.[1] It was found that the mode spectrum extends over the same frequency range as the magnetostatic mode spectrum of a spheroid,[2] namely from $\omega=\gamma H_i$ to $\omega=\gamma(H_i+2\pi M)$. It was also found that the spectrum of a slab clearly divides into two regions, one region extending from $\omega=\gamma H_i$ to $\omega=\gamma(B_iH_i)^{\frac{1}{2}}$ (coincident with the spin-wave band at long wavelengths[3]) in which the modes are spatially harmonic plane waves, and the other region from $\omega=\gamma(B_iH_i)^{\frac{1}{2}}$ to $\omega=\gamma(H_i+2\pi M)$ in which the modes are surface waves with exponentially decaying amplitude as one goes from the surface towards the interior of the ferromagnetic medium. The purpose of the present note is to show the general existence of surface modes in this frequency region immediately above the spin-wave band for uniformly magnetized samples of rather arbitrary shape and to discuss some of their properties. We find that not only may the magnetostatic mode spectrum in general be regarded as divided into volume and surface modes, but that the complete spin-wave spectrum similarly consists of a set of surface spin waves in addition to the usual spin-wave spectrum of an infinite medium.[3] Therefore, if one includes the surface spin waves, the magnetostatic mode spectrum merges smoothly into the total spin-wave spectrum.[4,5]

The general features of the surface modes may be derived by considering a semi-infinite ferromagnetic medium whose surface is at an angle, α, to the internal dc magnetic field, H_i, as shown in Fig. 1. (In the limit

[1] R. W. Damon and J. R. Eshbach, *Fifth Conference on Magnetism and Magnetic Materials, Detroit, Michigan, November 16–19, 1959* [J. Appl. Phys. (to be published)].
[2] L. R. Walker, Phys. Rev. **105**, 390 (1957).
[3] C. Herring and C. Kittel, Phys. Rev. **81**, 869 (1951).
[4] L. R. Walker, J. Appl. Phys. **29**, 318 (1958).
[5] C. R. Buffler, Suppl. J. Appl. Phys. **30**, 172S (1959); Robert L. White, Suppl. J. Appl. Phys. **30**, 182S (1959).